Protein Science

A PUBLICATION OF THE PROTEIN SOCIETY

SUSTAINED IN PART WITH THE SUPPORT OF THE AMERICAN SOCIETY FOR BIOCHEMISTRY AND MOLECULAR BIOLOGY
AND BY THE INNOVATIVE TECHNOLOGY FUND SUPPORTED BY THE BIOPHYSICAL SOCIETY

VOL. 1, NO. 6

JUNE 1992

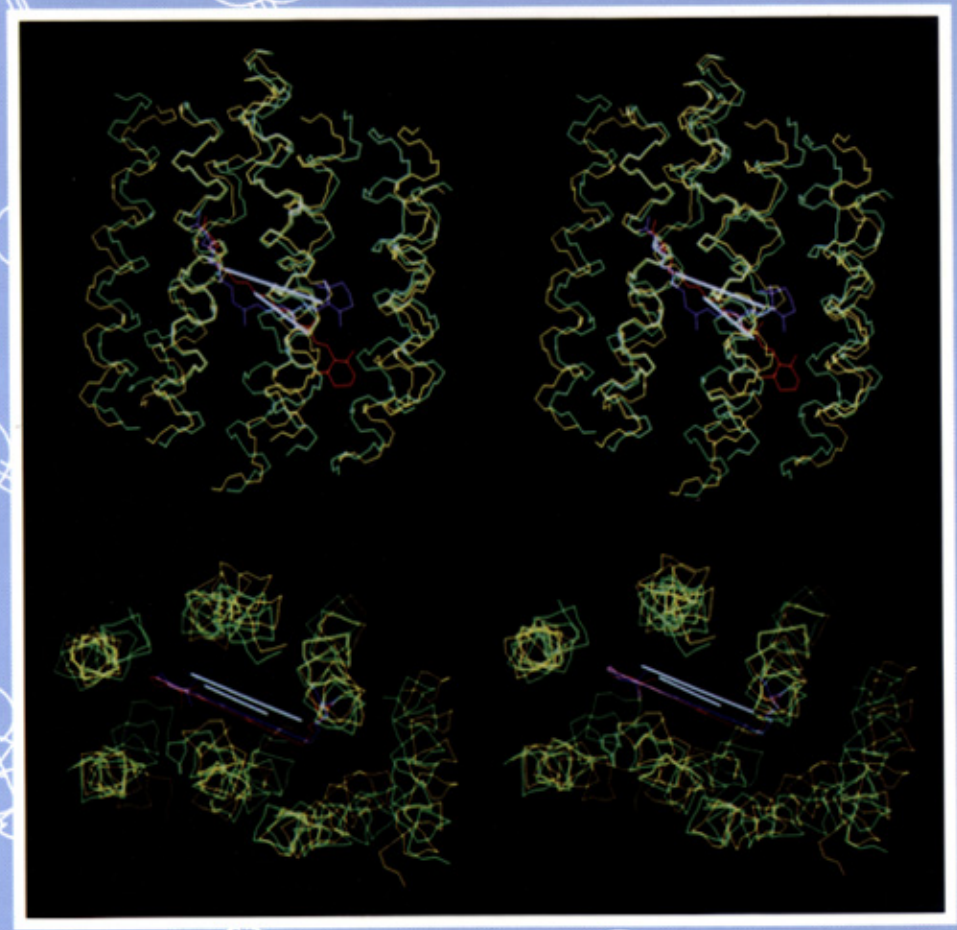

Cambridge University Press

Protein Science (1992), *1*, 810–827. Cambridge University Press. Printed in the USA.

An energy-based approach to packing the 7-helix bundle of bacteriorhodopsin

KUO-CHEN CHOU, LOUIS CARLACCI,[1] GERALD M. MAGGIORA, L.A. PARODI, AND M.W. SCHULZ

Computational Chemistry, Upjohn Laboratories, Kalamazoo, Michigan 49001

(RECEIVED December 4, 1991; REVISED MANUSCRIPT RECEIVED January 24, 1992)

Abstract

Based on the heavy-atom coordinates determined by the electron microscopy for the seven main helical regions of bacteriorhodopsin with the all-trans retinal isomer, energy optimizations were carried out for helix bundles containing the all-trans retinal and 13-cis retinal chromophores, respectively. A combination of simulated annealing and energy minimization was utilized during the process of energy optimization. It was found that the 7-helix bundle containing the all-trans isomer is about 10 kcal/mol lower in conformational energy than that containing the 13-cis isomer. An energetic analysis indicates that such a difference in energy is consistent with the observation that absorption of a 570-nm proton is required for the conversion of a bacteriorhodopsin from its all-trans to 13-cis form.

It was also found that the above conversion process is accompanied by a significant conformational perturbation around the chromophore, as reflected by the fact that the β-ionone ring of retinal moves about 5.6 Å along the direction perpendicular to the membrane plane. This is consistent with the observation by Fodor et al. (Fodor, S.P.A., Ames, J.B., Gebhard, R., van der Berg, E.M.M., Stoeckenius, W., Lugtenburg, J., & Mathies, R.A., 1988, *Biochemistry 27*, 7097–7101). Furthermore, it is interesting to observe that although the retinal chromophore undergoes a significant change in its spatial position, the orientation of its transition dipole changes only slightly, in accord with experimental observations. In other words, even though orientation of the retinal transition dipole is very restricted, there is sufficient room, and degrees of freedom, for the retinal chromophore to readjust its position considerably. This finding provides new insight into the subtle change of the retinal microenvironment, which may be important for revealing the proton-pumping mechanism of bacteriorhodopsin.

The importance of electrostatic and nonbonded interactions in stabilizing the 7-helix bundle structure has also been analyzed. Electrostatic interactions favor an antiparallel arrangement among adjacent helices. Nonbonded interactions, however, drive most of the closely packed helices into an arrangement in which the packing angles lie around −160°, a value very near the −154° value computed earlier as the most favorable packing arrangement of two poly(Ala) α-helices (Chou, K.-C., Némethy, G., & Scheraga, H.A., 1983, *J. Phys. Chem. 87*, 2869–2881).

The structural features of the 7-helix bundle and their relationship to those found in typical 4-helix bundle proteins are also discussed. The knowledge thus obtained suggests that many 7-helix membrane proteins might probably be built in a stepwise fashion from 4-helix bundle groups.

Keywords: all-trans and 13-cis bundles; energy minimization; packing of 7 helices; relation with 4-helix bundle; retinal chromophore and its microenvironment; simulated annealing; transition dipole

Bacteriorhodopsin (bR), a membrane protein that functions as a light-driven proton pump in *Halobacterium halobium* (Oesterhelt & Stoeckenius, 1973), is a single polypeptide with 248 amino acids; its sequence was first determined by Ovchinnikov et al. (1979) and Khorana et al. (1979). The study of bR has become an area of considerable interest in biochemistry (Lozier et al., 1975; Engelman & Zaccai, 1980; Engelman et al., 1980; Parodi et al., 1980; Nagle et al., 1982; Ovchinnikov 1982; Harbison et al., 1985; Fodor et al., 1988; Khorana, 1988; Kouyama et al., 1988; Lin & Mathies, 1989; Popot et al., 1989; Boehm et al., 1990; Henderson et al., 1990; Gebhard et al., 1991; Mathies et al., 1991). It is well known that bR is a photoreceptor that consists of a bundle of seven transmembrane helices, a structural feature shared by many integral membrane receptor proteins such as

Reprint requests to: Kuo-Chen Chou, Computational Chemistry, Upjohn Laboratories, Kalamazoo, Michigan 49001.

[1] Postdoctoral fellow in Upjohn Laboratories from July 1, 1988, to October 15, 1990. Present address: Department of Biochemistry & Biophysics, School of Medicine, University of Pennsylvania, Philadelphia, Pennsylvania 19104-6059.

those of the adrenergic, cholinergic, serotonin, dopamine, somatostatin, substance P, substance K, and angiotensin receptors (Dixon et al., 1988; Strader et al., 1989). As pointed out by Rao et al. (1983), the packing of seven helices together in integral membrane proteins may represent a uniquely stable arrangement that has been achieved through a process of convergent evolution, and thus it is expected that more examples of such proteins will appear in the future. Hence, the study of the packing of 7-helix bundle transmembrane-protein domains based on energetics will be of general applicability and should provide many useful insights that will aid efforts to understand the structures and functions of not only bR but also many other 7-helix bundle proteins.

Recently, the heavy-atom coordinates of heavy atoms of the seven main helical regions in bR were determined by high-resolution electron cryomicroscopy (Kinemage 1; Henderson et al., 1990). The structure has 10 Å resolution perpendicular and 3.5 Å resolution parallel to the membrane plane. Because of the limited vertical resolution no atomic coordinates for the loop regions could be determined. In addition, although the positions of the side chains in the helical regions are clear, their precise conformations have not been determined reliably, and thus it is worthwhile to refine the 7-helix structure via energy optimization. Furthermore, as is well known, bR contains one molecule of all-trans retinal bound to Lys 216 (on helix G) via a protonated Schiff-base linkage; light absorption brings about, through a series of steps, isomerization of all-trans retinal to its 13-cis isomer. This results in proton transport across the bacterial membrane, from the inside to the outside of the *H. halobium* cell (Oesterhelt & Stoeckenius, 1973; Fodor et al., 1988; Khorana, 1988). Thus, it is important to any detailed understanding of the proton-pumping mechanism that the nature of the conformational change in bR brought about by photoisomerization be determined. As the atomic coordinates determined by the electron microscopy apply only to the all-trans retinal isomer, an effort was made in the current study to predict the conformation of the 7-helix bundle with the 13-cis retinal isomer.

Nomenclature

For the sake of succinctness, the following terminologies are used in this paper:

$$\left.\begin{aligned} \text{all-trans bR} &\equiv \text{bacteriorhodopsin with all-trans retinal chromophore;} \\ \text{13-cis bR} &\equiv \text{bacteriorhodopsin with 13-cis retinal chromophore;} \\ \text{all-trans bundle} &\equiv \text{the 7-helix bundle in the all-trans bR;} \\ \text{13-cis bundle} &\equiv \text{the 7-helix bundle in the 13-cis bR.} \end{aligned}\right\} \quad (1)$$

The retinal chromophore is attached to Lys 216 of bR via a Schiff-base linkage. The Schiff base of all-trans bR is always protonated, while the Schiff base of 13-cis bR is sometimes protonated, such as in the K, L, and O states, and sometimes unprotonated, such as in the M and N states (Khorana, 1988). Or, according to Schulton and Tavan (1978) and Fahmy et al. (1989) the conformations of retinal in most intermediate states are not yet known for sure to be 13-cis or 13,14-dicis. Nevertheless, it is known that the deprotonation state M is 13-cis, and also among these intermediate states the M state is the longest lived and the most important one for the kinetic study of bR. Therefore, in the current investigation, in addition to the all-trans bR with protonated Schiff base, only the 13-cis bR with unprotonated Schiff base is considered. In view of this, we can, in a broad sense, treat the all-trans retinal-lysine and 13-cis retinal-lysine as two additional amino acids, whose three-letter codes were given by (Carlacci et al., 1991b):

$$\left.\begin{aligned} \text{Krt}^+ &\equiv \text{all-trans retinal-lysine with protonated Schiff base;} \\ \text{Krc} &\equiv \text{13-cis retinal-lysine with unprotonated Schiff base.} \end{aligned}\right\} \quad (2)$$

The geometric and energy parameters for Krt^+ and Krc were provided in Carlacci et al. (1991b).

The standard conventions for the nomenclature of polypeptide conformations have been followed (IUPAC-IUB Commission on Biochemical Nomenclature, 1970).

Mathematical and physical formulation

In this section a brief description is presented of some of the mathematical and physical quantities useful in characterizing the 7-helix bundle structure.

Internal and external variables

To uniquely describe the atomic coordinates of a multiple chain system, such as the 7-helix bundle in bR, two types of parameters are needed, i.e., internal and external variables. The former describes the conformation of a polypeptide chain in terms of a set of dihedral angles, or torsional angles, such as ϕ, ψ, ω, χ, ..., whereas the latter describes the relative position and orientation among the helices in terms of a set of rigid-body variables. In dealing with a multiple helix system, it is convenient to adopt the (f, g, h) helical coordinate system defined by Chou et al. (1984), in which the coordinate of any atom in the mth polypeptide chain can be expressed by the following equation:

$$\mathbf{r}_m = \mathbf{\Omega}_m \cdot \mathbf{r}'_m + \mathbf{t}_m, \quad (3)$$

where $\mathbf{t}_m = (t_f, t_g, t_h)_m$ is the translation vector of the mth chain and $\mathbf{\Omega}_m$ the corresponding unitary rotation matrix is given by Equation 4 (below), where α_m, β_m, and γ_m are the Euler angles for the mth chain as defined in Chou et al. (1984). In Equation 3, $\mathbf{r}'_m$ denotes the coordinates of any atom in the mth chain when it is in the reference position, i.e., the position corresponding to $\alpha_m = \beta_m = \gamma_m = 0$ and $\mathbf{t}_m = 0$, meaning that the axis of the mth chain (defined by the least-square line through its C^α atoms) and its center coincide with the h-axis and the origin of the (f,g,h) coordinate system, respectively. (See Chou et al. [1984] for a detailed description about the reference position and the (f,g,h) coordinate system.) The vector $\mathbf{r}_m$ denotes the coordinates of the same atom after the mth chain has been rotated and translated from its reference position as described by Equations 3 and 4.

Description of packing angles

In the study of helix/helix packing, the relative orientation of two packed structures is usually expressed in terms of an orientation angle (Chothia et al., 1977, 1981; Chou et al., 1984, 1990), denoted by Ω_0, which measures the tilting of the helix axes, with $\Omega_0 = 0°$ for parallel and $\Omega_0 = \pm 180°$ for antiparallel orientations, respectively. The orientation angle is positive if, starting from an initial parallel orientation of the helices ($\Omega_0 = 0°$), the helix furthest from the viewer is rotated clockwise relative to the one nearest to the viewer; it is negative if the furthest helix is rotated in the counterclockwise sense. Expressed in terms of unit vectors $\mathbf{e}_i$ and $\mathbf{e}_j$, which coincide with the helix axes (Chou et al., 1984) and point from the N- toward the C-terminus of each helix,

$$\Omega_0 = \begin{cases} \cos^{-1}(\mathbf{e}_i \cdot \mathbf{e}_j) & \text{for clockwise rotation} \\ -\cos^{-1}(\mathbf{e}_i \cdot \mathbf{e}_j) & \text{for counterclockwise rotation.} \end{cases} \tag{5}$$

The sign and magnitude of Ω_0 are independent of which helix is chosen as the nearest or furthest.

Energy calculations

Energy calculations were carried out with ECEPP/2 (Némethy et al., 1983), which is an updated version of the original ECEPP (empirical conformational energy program for peptides) developed by Momany et al. (1975). However, the energies involving retinal chromophore were calculated with the augmented ECEPP system (Carlacci et al., 1991b), which is expanded from ECEPP to cover some key elements in retinal-containing proteins and treat them as additional amino acids, such as those symbolized by Krt^+ and Krc (see Equation 2). The total energy of a set of packed polypeptide chains is the sum of the intrachain and all interchain energies (Chou et al., 1985, 1986) and is given by

$$E^{tot} = \sum_m E^m_{intra} + \sum_m \sum_{n<m} E^{mn}_{inter}, \tag{6}$$

where E^m_{intra} is the intrachain energy of the mth chain and E^{mn}_{inter} is the interchain energy between chains m and n. The energy is computed as the sum of electrostatic, nonbonded (van der Waals), hydrogen-bonded, and torsional energies (Momany et al., 1975; Némethy et al., 1983).

Definition of helix–helix contacts

Although the interaction between α-helices is described quantitatively by their interaction energy, an approximate geometrical measure of interaction between two α-helices can be given by specifying the number of pairs of atoms or of residues that are in contact. In particular, information derived from these data will provide an intuitive and detailed picture of the internal microenvironment of the 7-helix bundle, which is useful for studying the proton-pumping mechanism of bR (Mogi et al., 1988). These numbers are computed based on atomic van der Waals radii, according to a method defined earlier (Chou et al., 1983). Their significance and limitations have been discussed (Chou et al., 1984).

Two atoms i and j, located in different α-helices, are defined to be in contact if the distance d between them is less than a cutoff distance d^*, i.e., if

$$d < d^* = (2 - 2^{-1/6})(r_i^\circ + r_j^\circ), \tag{7}$$

where r_i° and r_j° are the respective van der Waals radii, and the coefficient $(2 - 2^{-1/6})$ is the result of considering the fluctuation of the atom pair around their van der Waals contact distance. (See Chou et al. [1983] for the detail of the derivation of Equation 7 and for the numerical values of r°.)

Two residues, from different helices, are defined to be in contact if they have at least one pair of atoms in contact, as defined by Equation 7.

$$\mathbf{\Omega}_m = \begin{bmatrix} \cos\alpha_m \cos\gamma_m - \sin\alpha_m \cos\beta_m \sin\gamma_m & -\cos\alpha_m \sin\gamma_m - \sin\alpha_m \cos\beta_m \cos\gamma_m & \sin\alpha_m \sin\beta_m \\ \sin\alpha_m \cos\gamma_m + \cos\alpha_m \cos\beta_m \sin\gamma_m & -\sin\alpha_m \sin\gamma_m + \cos\alpha_m \cos\beta_m \cos\gamma_m & -\cos\alpha_m \sin\beta_m \\ \sin\beta_m \sin\gamma_m & \sin\beta_m \cos\gamma_m & \cos\beta_m \end{bmatrix} \tag{4}$$

Computational methods

The computational procedure consists of the following two parts, described below: (1) generation of the initial structures for the all-trans bundle and 13-cis bundle, in which the N- and C-terminal groups for each of the constituent helices are H_2N- and $-COOH$, respectively, and (2) energy optimization of each of the two structures. The computations were carried out on an IBM 3090/400J computer at Upjohn Laboratories.

Generation of initial 7-helix bundles

The initial all-trans bundle

Appropriate internal and external variables (see section on Internal and external variables, earlier) were generated based on the heavy-atom coordinates determined by Henderson et al. (1990) for the seven main helical regions of bR (see Fig. 1). The heavy-atom root mean square (rms) value between the structure thus generated and that determined by high-resolution electron cryomicroscopy (Henderson et al., 1990) was about 0.2 Å. Dihedral angles related to positions of hydrogen atoms were assigned according to data on energy-minimized amino acid residues (Vásquez et al., 1983), and are called assigned dihedral angles. The arbitrariness of their conformations was removed by subsequent energy minimization (see Adjustment of the assigned dihedral angles, below). The retinal-Lys 216 moiety at helix G was generated by replacing Lys 216 with Krt^+ 216 (see Equation 2) with the appropriate parameters provided in the augmented ECEPP system (Carlacci et al., 1991b). Because the Krt^+ is pro-

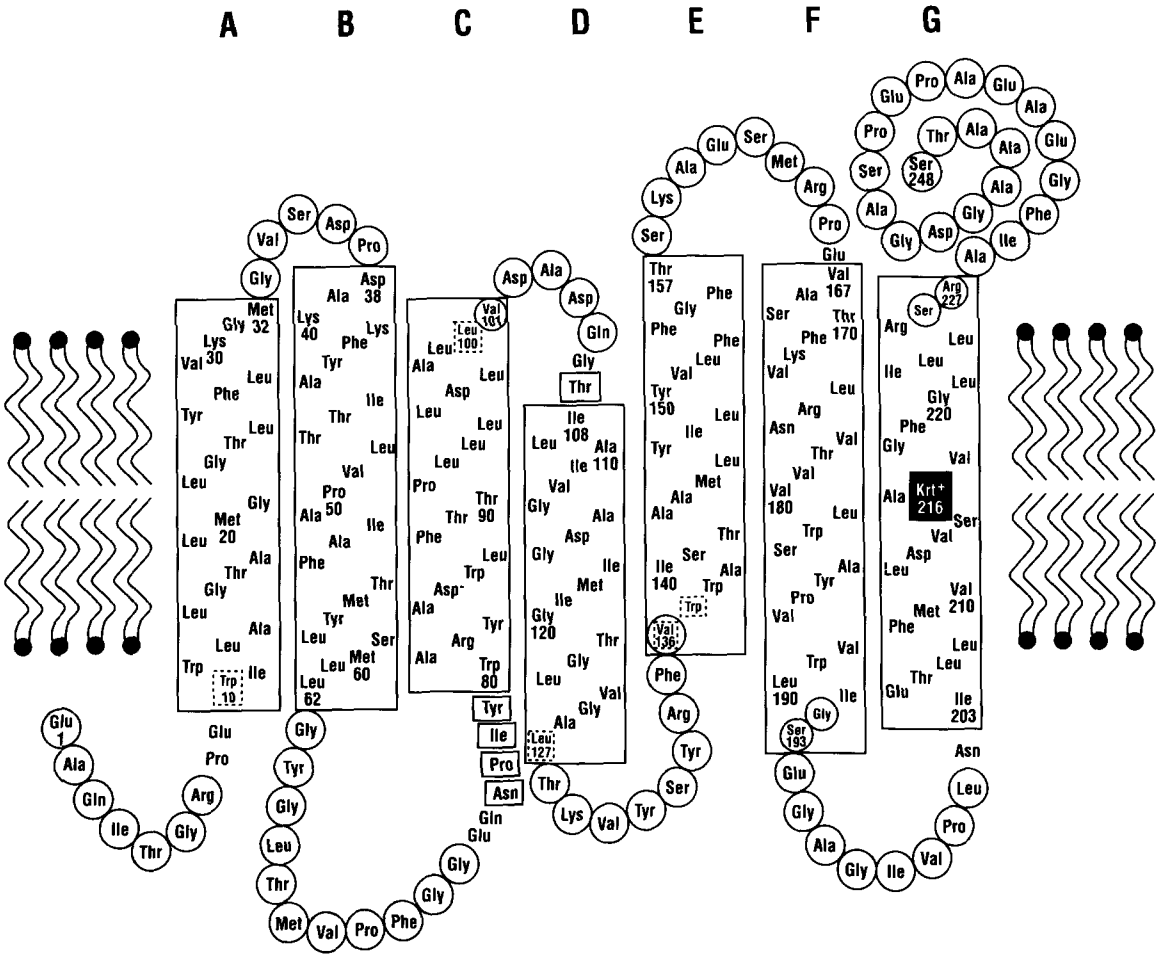

Fig. 1. A secondary structure model of bacteriorhodopsin with the all-trans retinal chromophore (abbreviated as the all-trans bR). This model is based on the results determined by Henderson et al. (1990) in terms of high-resolution electron cryomicroscopy. The helical segments assigned by them are outlined by a cylinderlike box. Residues within a circle are those whose heavy-atom coordinates have not been determined yet. The cytoplasm is at the top. The all-trans retinal chromophore is attached to Lys 216 of helix G via a protonated Schiff-base linkage. Such a retinal-lysine isomer is represented by Krt^+ (Carlacci et al., 1991b). Residues within a solid-line box are those that, after energy optimization, moved into a helical region from a nonhelical region, whereas residues within a dotted-line box are those with just the opposite conversion. The left side and right side of the protein secondary structure are the schematic representation for the cytoplasmic membrane into which the bR is embedded. The capital letters A, B, ..., G at the top of the figure label the helices.

tonated, Asp^- 85 (Mogi et al., 1988) was taken as the corresponding deprotonated "conjugate" residue, in which the carboxyl group has the form of COO^- to maintain the electroneutrality of the entire system for calculation.

The initial 13-cis bundle

The initial 13-cis bundle was generated from the all-trans bundle by substituting Krc for Krt^+ at the appropriate position in helix G and Asp for Asp^- at the appropriate position in helix C. If the substitution, however, is made by simply replacing Krt^+ by Krc without any adjustment in the side-chain dihedral angles, this will result in a flip-flop in direction for the polyene chain of the retinal moiety (Carlacci et al., 1991b), with a shift of ~18 Å for the β-ionone ring therein. On the other hand, experimental observations (Parodi et al., 1980; Lin & Mathies, 1989; Ding et al., 1990) indicate that the polyene chains of the retinal moieties in all-trans and 13-cis bR are pointing to almost the same direction, i.e., toward the cytoplasmic surface. Therefore, it would be wise to make some adjustments to the side-chain dihedral angles during the substitution so as to generate an appropriate geometry for the chromophore in the initial 13-cis bundle. This was accomplished through MOSAIC, the Upjohn molecular modeling system (Howe et al., 1992), which allowed us to manipulate Krc 216 on screen to ensure that its polyene chain has the same general direction as that of Krt^+ 216 has in the all-trans bundle. It was found that the side-chain dihedral angles χ^1, χ^2, χ^3, χ^4, and χ^5 of the Krc moiety (Carlacci et al., 1991b) should be adjusted from −31°, 162°, 112°, 97°, and −113° to −12°, 152°, 102°, 128°, and −113°, respectively, when Krt^+ in the all-trans bundle is replaced with Krc for generating the initial 13-cis bundle. Through the above adjustment for the direction of the polyene chain in the 13-cis bundle, the shift in the β-ionone ring of retinal between the all-trans and 13-cis bundles is accordingly reduced from ~18 Å to 4.6 Å. Although such an adjustment could also be fulfilled using simulated annealing (Chou & Carlacci, 1991), the approach described here is far easier and provides an appropriate starting structure for further studies.

Energy minimization procedure

The initial structures of the two 7-helix bundles generated as described above were then subjected to energy minimization.

The energy minimizations were carried out with the PACK/2 program, which was developed by Carlacci and Chou (1991), and was based on the original program PACK established for energetic approach to the helix/helix (Chou et al., 1984), helix/sheet (Chou et al., 1985), and sheet/sheet packing (Chou et al., 1986) studies in proteins. In PACK/2 the finite difference estimation of the gradient of the potential energy is replaced by an analytical gradient, which significantly enhances the efficiency of energy minimization for a multiple chain system. In addition, in contrast to the PACK program in which one chain was held fixed during the minimization, in PACK/2 all chains are allowed to rotate and translate. This provides an additional advantage of increasing the flexibility of a packed structure by allowing concerted movement of all the polypeptide chains. Furthermore, at the early stage of energy minimization, simulated annealing (see Simulated annealing) and energy minimization were alternately applied in order to avoid the possibility that the energy-minimized structure may become trapped in a local minimum.

The energy optimization was carried out in the following three successive steps:

Adjustment of the assigned dihedral angles

The energies of the all-trans bundle and 13-cis bundle were minimized only with respect to all the assigned dihedral angles, i.e., those torsional angles corresponding to hydrogen atoms (see The initial all-trans bundle). The reason to handle these angles first is that their initial values were assigned somewhat arbitrarily because no experimental data are available in locating them. Energy minimization of this step involved 224 and 225 independent variables, respectively, for the all-trans and 13-cis bundles, whose optimization would eliminate atomic overlaps caused by the initial assignment.

Simulated annealing

The 7-helix bundles obtained from the above step were subjected to simulated annealing treatment, which consists of the following two steps: (1) simulated annealing with respect to the $6 \times 7 = 42$ rigid-body variables, i.e., α, β, γ, t_f, t_g, t_h for each of the seven helices (see Equations 3 and 4), and (2) simulated annealing with respect to all the side-chain angles. This procedure was adopted in order to avoiding being trapped in local minima and thus to increase the likelihood of finding the global energy minimum. It is particularly important for the 13-cis bundle where experimental data are as yet unavailable. The initial conformation of the 13-cis bundle was derived from that of the all-trans bundle as described earlier (see Generation of initial 7-helix bundles). However, such a procedure may not be entirely satisfactory due to the possibility that a large conformational change, thought of as a "proteinquake" by Fodor et al. (1988), might occur in bR when its retinal chromophore is converted from its all-trans to its 13-cis isomer. Therefore, the initial conformation (vide supra) of the chromophore of the 13-cis bundle is very likely in or near a local minimum. Even for the all-trans bundle, this is likely to be the case because the experimental data from which the initial conformation was generated have a limited vertical resolution, as reflected by the fact that the N- and C-terminal residue numbers are uncertain by at least one residue (Henderson et al., 1990). Simulated annealing with respect to the rigid-body

variables would be particularly helpful in overcoming the local minimum problem incurred by such an uncertainty along the vertical direction (Chou & Carlacci, 1991).

Recently, a program, SAPK (simulated annealing for packing), was developed to help overcome the local minimum problem in packed protein structures (Chou & Carlacci, 1991). The relevant parameters used by SAPK to treat rigid-body minimizations were: the starting temperature $T^\circ = 5.0 \times 10^4$ K, the cooling factor $\lambda = 1.5$, the cooling steps $\mu = 30$, and the central processing unit (CPU) time (for IBM 3090 computer) assigned to each of the 30 temperatures for the random conformation-sampling process was 0.2 h, i.e., the total CPU time for the whole annealing process in each such treatment was $0.2 \times 30 = 6$ h. The corresponding parameters for the simulated annealing treatment of the side-chain dihedral angles were: the starting temperature $T^\circ = 2.5 \times 10^4$ K; the cooling factor $\lambda = 1.5$, the cooling steps $\mu = 20$, and the CPU time (for IBM 3090 computer) assigned to each of the 30 temperatures for the random conformation-sampling process was 0.5 h, i.e., the total CPU time for the whole annealing process in each such treatment was $0.5 \times 20 = 10$ h.

Energy minimization

For each of the helix bundles obtained through the above procedure, the program PACK/2 was used to carry out energy minimization in the following three successive steps. In the first step, all backbone dihedral angles and rigid-body variables were kept fixed, and the energy was minimized with respect to the side-chain dihedral angles only, i.e., 476 variables for the case of the all-trans bundle and 477 variables for the case of the 13-cis bundle, in order to eliminate bad atomic overlaps. In the second step, only the rigid-body variables were fixed, but all dihedral angles were allowed to vary; the numbers of independent variables were increased to 979 and 980, respectively. Finally, in the third step, no constraint was imposed, and the energy was minimized with respect to all dihedral angles and all rigid-body variables, i.e., 1,021 and 1,022 independent variables for the all-trans and 13-cis bundles, respectively. Preliminary tests indicated that the present procedure significantly improves the computational efficiency of the structure determination process.

Quantum chemical calculations

The transition dipole of a structure can be used to indicate its orientation. In this paper, the transition dipoles of retinal chromophores were calculated with the program developed by Ridley and Zerner (1973) based on the INDO (intermediate neglect of differential overlap) theory established by Pople et al. (1967).

The flow chart given in Figure 2 provides an overview of the entire model building process employed here.

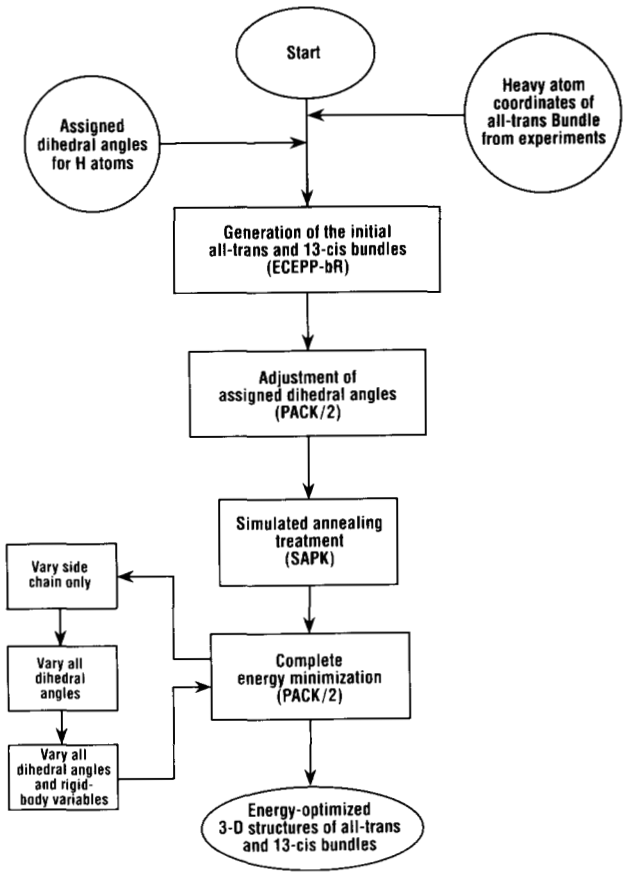

Fig. 2. A flow diagram showing an overview of the entire model building process used here. The program names are in parentheses.

Results and discussion

The geometric and energy parameters characterizing each of these energy-optimized 7-helix bundles are listed in Tables 1–6. Stereo drawings illustrating various features of these two structures are given in Figures 3–6. A detailed analysis of the results is presented below.

General structural features

The position and orientation of each constituent chain, as described by α, β, γ, t_f, t_g, t_h, and its intrachain energy are listed in Table 1. Table 2 contains data describing the relations and interactions between any two chains in each of the two 7-helix bundles, especially the distance of closest approach D (Chou et al., 1983), packing angle Ω_0, interchain energy (in electrostatic term and nonbonded term), number of atom pairs in contact, and number of residue pairs in contact. It is interesting to note from Table 2 that for most of the closely packed helix pairs (i.e., $D \leq 11$ Å), such as the A–B, B–C, B–G, D–E, E–F, and F–G pairs in the all-trans bundle and the A–B, B–C, C–D, D–E, E–F, and F–G pairs in the 13-cis

Table 1. *Parameters characterizing each of the constituent chains in the energy-optmized all-trans and 13-cis bundles, respectively*

Type of bundle	Helix	Euler angles (degrees)			Translation (Å)			Intrachain energy E_{intra} (kcal/mol)
		α	β	γ	t_f	t_g	t_h	
All-trans	A	58	19	−60	12.7	6.4	−0.5	−60.61
	B	113	165	41	10.4	−2.0	3.2	−31.19
	C	−89	13	9	2.0	−4.6	−3.1	−112.57
	D	150	169	−23	−6.0	−10.3	−4.2	−42.55
	E	176	19	107	−13.5	−3.5	2.4	−42.10
	F	−32	168	144	−7.6	5.9	2.8	−78.60
	G	61	9	87	2.1	8.0	−0.6	−81.29
13-cis	A	56	24	−59	11.9	9.2	−1.3	−63.86
	B	143	171	75	10.0	0.9	2.7	−25.23
	C	−97	9	30	2.3	−4.0	−2.8	−150.45
	D	89	168	−93	−2.6	−12.6	−4.5	−43.18
	E	−165	8	95	−12.6	−7.2	2.6	−60.47
	F	−6	166	162	−9.2	4.9	3.7	−88.52
	G	74	9	91	0.2	8.8	−0.4	−97.56

bundle, the corresponding orientational angles are close to $\Omega_0 = -160° \pm 10°$. This is near the value computed earlier for the most favorable packing arrangement of two poly(Ala) α-helices (Chou et al., 1983), $\Omega_0 = -154°$, and to the values determined by numerous workers (see, e.g., Chothia & Finkelstein, 1991) for helix pairs in real proteins.

As shown in Figure 3 and Kinemage 1, there is a bend

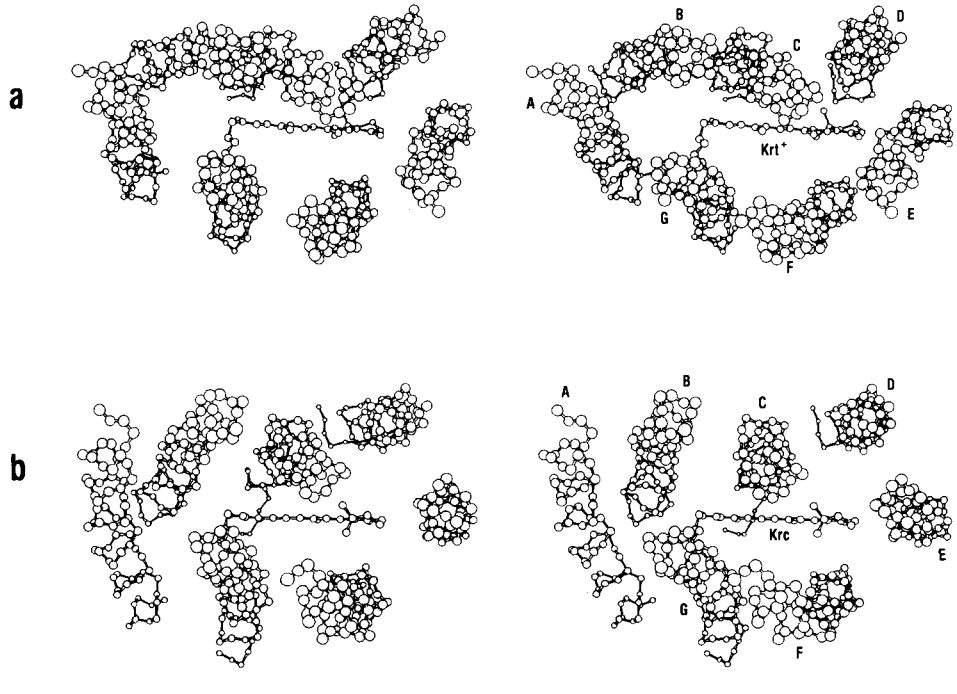

Fig. 3. The stereo stick-ball drawing of the energy-optimized 7-helix bundle: **(a)** the all-trans bundle, and **(b)** the 13-cis bundle. Only backbone atoms of the seven helices and the heavy atoms of retinal-lysine in helix G, i.e., Krt^+ in a and Krc in b, are shown. The proton attached to the Schiff base of Krt^+ is also included in a although it is not very remarkable. The bend in helices B, C, and F is caused by the existence of a proline in each of these three helices: Pro 50 in helix B, Pro 91 in helix C, and Pro 186 in helix F (cf. Fig. 1). Viewed from the cytoplasmic surface, the β-ionone ring of the retinal in b is about 5.6 Å closer to the viewer than that in a. However, the retinal polyene chains in both cases are pointing to almost the same direction, i.e., toward the extracellular surface.

Table 2. *Parameters characterizing packing interactions in the energy-optimized all-trans and 13-cis bundles*

Type of bundle	Helix pair		Distance of closest approach D (Å)	Orientation angle Ω_0 (degrees)	Interchain energy (kcal/mol)			Number of atom pairs in contact	Number of residue pairs in contact
	In contact	Not in contact			E_{inter}^{ES}	E_{inter}^{NB}	E_{inter}		
All-trans	A-B		8.1	−150	−5.02	−62.70	−67.72	412	24
	A-C		14.0	30	1.21	−5.06	−3.85	20	2
		A-D	21.5	−159	−0.97	−0.08	−1.05	0	0
		A-E	28.0	32	0.61	−0.04	0.57	0	0
		A-F	19.0	−158	−1.52	−0.34	−1.86	0	0
	A-G		8.2	10	5.44	−36.89	−31.45	233	15
	B-C		9.3	−170	−6.04	−47.40	−53.44	274	23
		B-D	18.2	−9	1.45	−0.39	1.06	0	0
		B-E	20.4	−151	−1.02	−0.13	−1.15	0	0
		B-F	17.5	26	1.91	−0.75	1.16	0	0
	B-G		10.4	−158	−3.03	−9.44	−12.47	33	5
	C-D		9.9	168	−3.83	−39.14	−42.97	228	21
	C-E		12.1	23	1.49	−6.26	−4.77	37	3
	C-F		13.1	−158	−0.90	−16.35	−17.25	55	9
	C-G		12.4	21	−29.80	−36.37	−66.17	210	15
	D-E		8.5	−151	−2.92	−28.64	−31.56	154	17
	D-F		11.8	23	2.46	−6.44	−3.98	30	3
	D-G		17.7	−166	−1.59	−8.30	−9.89	39	2
	E-F		9.9	−169	−2.54	−44.92	−47.46	256	21
	E-G		18.4	24	2.37	−5.47	−3.10	36	3
	F-G		10.2	−165	−7.33	−64.68	−72.01	364	24
13-cis	A-B		7.8	−154	−4.90	−60.00	−64.90	397	26
		A-C	16.1	33	1.93	−1.71	0.22	0	0
		A-D	25.9	−145	−0.79	−0.05	−0.84	0	0
		A-E	28.9	30	0.63	−0.03	0.60	0	0
		A-F	20.2	−147	−1.57	−0.23	−1.80	0	0
	A-G		9.0	16	5.10	−25.40	−20.30	112	11
	B-C		9.7	−169	−4.52	−42.21	−46.73	284	21
		B-D	19.3	10	1.50	−0.35	1.15	0	0
		B-E	22.0	−165	−1.04	−0.12	−1.16	0	0
		B-F	19.4	22	2.04	−0.61	1.43	0	0
	B-G		10.8	−165	−4.06	−15.50	−19.56	70	6
	C-D		9.4	−170	−3.40	−40.78	−44.18	244	20
	C-E		12.4	10	2.52	−4.92	−2.40	18	2
	C-F		13.5	−163	−3.52	−17.11	−20.63	104	10
	C-G		12.1	18	3.25	−32.54	−29.29	168	13
	D-E		9.5	−167	−2.17	−19.23	−21.40	89	12
		D-F	15.9	20	1.29	−1.36	−0.07	0	0
	D-G		21.6	−159	−0.98	−3.12	−4.10	17	1
	E-F		10.1	−170	−2.57	−29.17	−31.74	163	14
	E-G		20.5	14	1.22	−6.07	−4.85	53	2
	F-G		10.5	−162	−6.32	−61.65	−67.97	302	26

in helices B, C, and F, which is due to the presence of a proline residue in each of these helices: Pro 50 in helix B, Pro 91 in helix C, and Pro 186 in helix F (Fig. 1).

The heavy-atom rms deviation between the energy-optimized all-trans bundle and the structure determined by Henderson et al. (1990) is 1.6 Å. The heavy-atom rms deviation between the energy-minimized all-trans bundle and 13-cis bundle is 2.4 Å (animated in Kinemage 2). The corresponding rms value between the retinal chromophores in the two energy- minimized bundles is 3.1 Å, implying that photoisomerization is accompanied by a significant conformational perturbation around the chromophore. This can also be seen in Figure 4: as a result of such a process, the β-ionone ring of retinal moves up about 5.6 Å along the direction perpendicular to the membrane plane. Such a large conformational change is consistent with the work of Fodor et al. (1988) where, based on time-resolved resonance Raman spectra, these authors have suggested that a "proteinquake" may occur. Similar phenomena in other biomacromolecules, such as

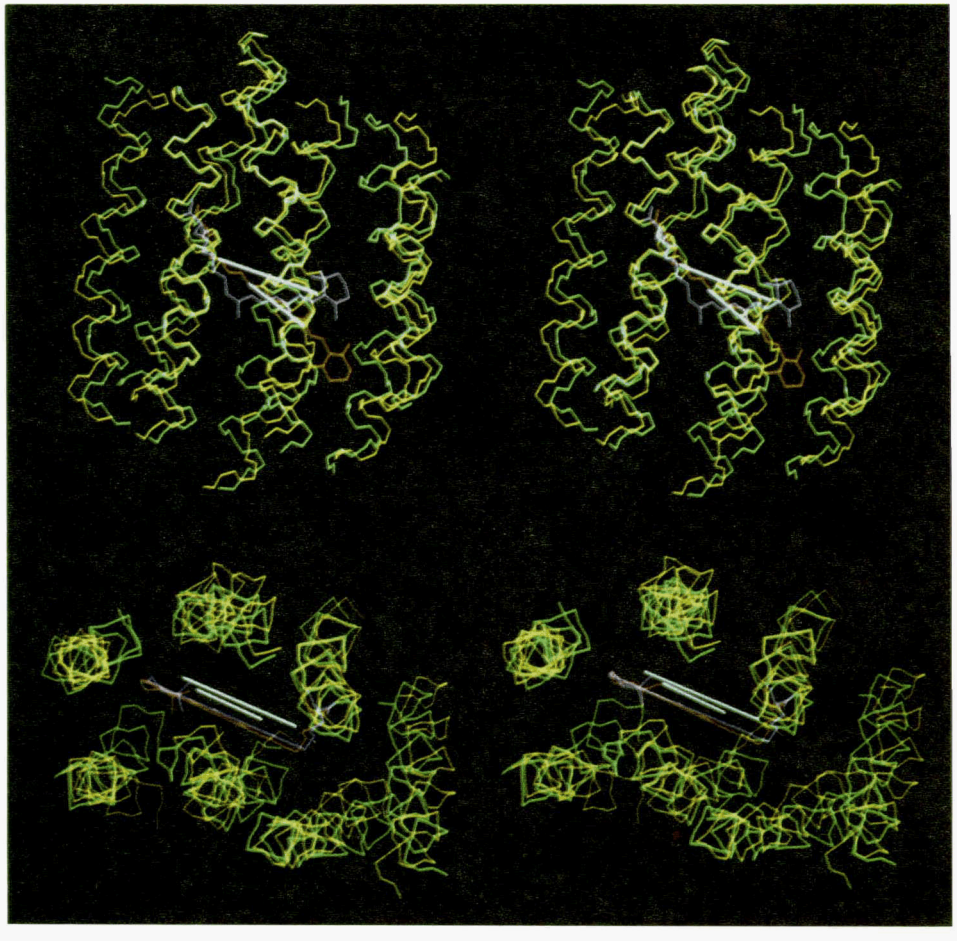

Fig. 4. Stereo backbone trace drawings of the energy-optimized all-trans and 13-cis bundles. All the heavy atoms of retinal-lysine in helix G and the proton of the protonated Schiff base in the all-trans bundle are also included. The all-trans bundle is drawn in green and its lysine-retinal in red. The 13-cis bundle is drawn in yellow and its lysine-retinal in purple. The upper white bar represents the transition dipole of the retinal isomer in the 13-cis bundle, and the lower one represents that in the all-trans bundle. The two structures have been superimposed in order to show the remarkable change (~5.6 Å) in the position of the β-ionone ring of retinal and only a trivial change in the orientation of the retinal transition dipole. **a**: Viewed from side of the bundle, with the cytoplasmic surface at the top. **b**: Viewed from top of the bundle, with cytoplasmic surface closer to the viewer. See the legend to Figure 3 for a further explanation.

the local "quakelike" motions in DNA, were recently discussed by Chou and Maggiora (1988) and Chou and Mao (1988) for the process of DNA–drug intercalation.

Interestingly, although the β-ionone ring experiences a significant change in its position during the all-trans to the 13-cis photoisomerization process, in both structures the retinal bears the following two common features: (1) the orientation of the transition dipole of the intense, long wavelength singlet–singlet transition, $S_1(\Pi,\Pi^*) \leftarrow S_0$, remains substantially unchanged (Fig. 4a), maintaining an angle of ~20° with respect to the membrane plane as observed (Heyn et al., 1977; Lin & Mathies, 1989), and (2) the plane of its chromophore is nearly perpendicular to the membrane plane (Fig. 4b), as observed (Earnest et al., 1986; Fahmy et al., 1989). Two bars are explicitly shown in white in Figure 4: the upper one represents the $S_1(\Pi,\Pi^*) \leftarrow S_0$ transition dipole of the retinal isomer in the 13-cis bundle, and the lower one represents the corresponding transition dipole in the all-trans bundle. These two transition dipoles were calculated with the program as described in Quantum chemical calculations. It can be seen from the figure that the orientation angle between

Table 3. *Energies of the computed all-trans and 13-cis bundles*

Type of bundle	Total intrachain energy,[a] E_{intra}^{tot} (kcal/mol)	Total interchain energy,[b] E_{inter}^{tot} (kcal/mol)	Total energy,[c] E^{tot} (kcal/mol)
All-trans	−448.91	−469.39	−918.30
13-Cis	−529.27	−378.55	−907.82

[a] Total intrachain energy E_{intra}^{tot} is the sum of terms in column 9 of Table 1.

[b] Total interchain energy E_{inter}^{tot} in the sum of terms in column 8 of Table 2.

[c] Total energy $E^{tot} = E_{intra}^{tot} + E_{inter}^{tot}$ as defined in Equation 6.

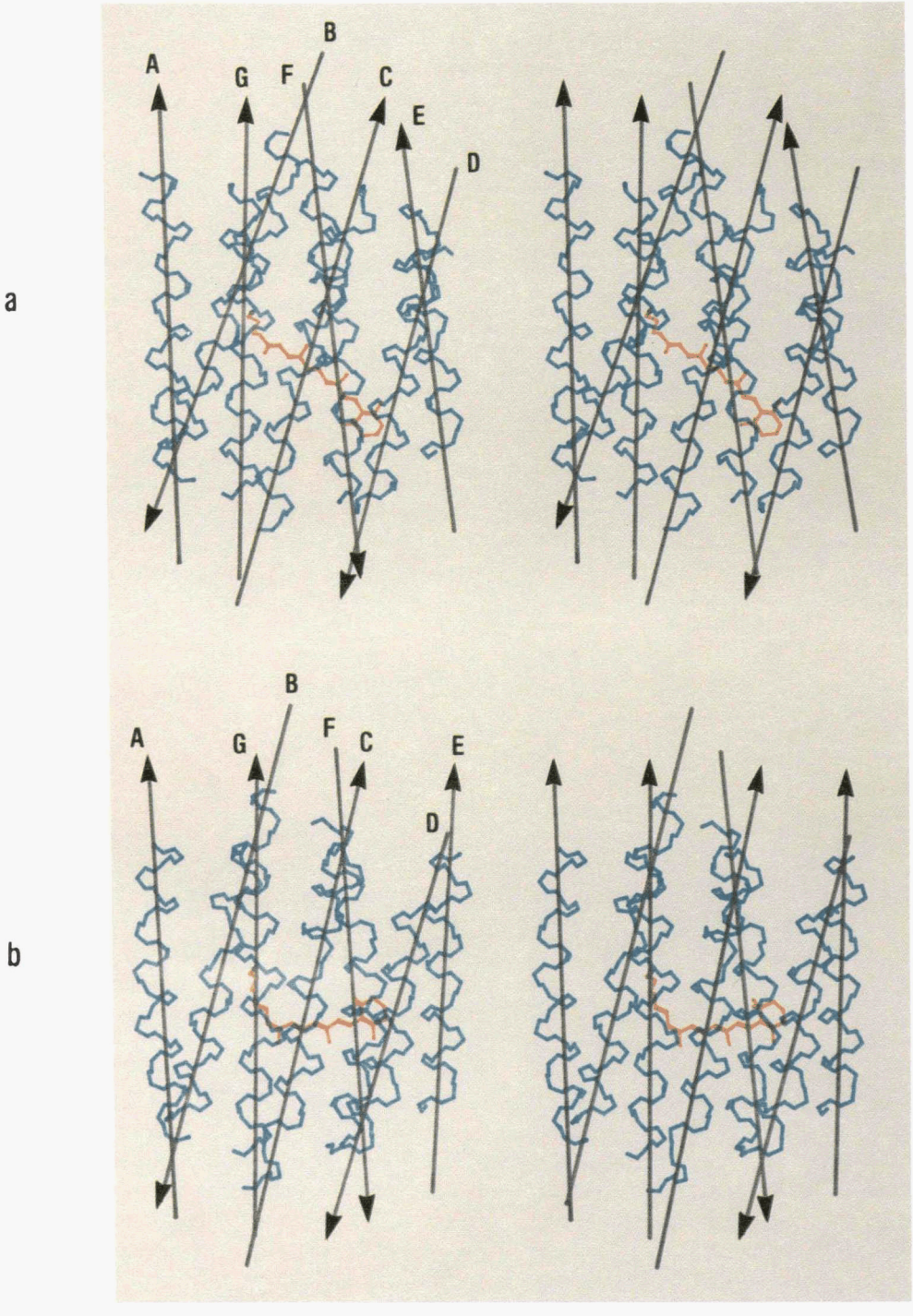

Fig. 5. The stereo backbone trace drawings of the energy-optimized 7-helix bundle: (**a**) the all-trans bundle, and (**b**) the 13-cis bundle. The blue line is the trace of the helix, the red line is the trace of the retinal-lysine, and the black line represents the axis of each helix as defined in Chou et al. (1984). Arrows indicating the helix axes point from the N to the C terminus. It can be seen in both bundles that: helices B, C, F, G form a typical antiparallel left-twisted 4-helix bundle as observed in most of the observed 4-helix proteins (Argos et al., 1977; Weber & Salemme, 1980; Richardson, 1981; Sheridan et al., 1982; Chou et al., 1988); helices A, B, C, G and helices C, E, F, G each form a mixed left-twisted 4-helix bundle, in which two adjacently antiparallel helix pairs are mixed with two adjacently parallel helix pairs but the whole structure is left-twisted; and helices C, D, E, F form an antiparallel quasi-left-twisted 4-helix bundle, in which one orientation angle, i.e., the one between helices C and D, deviates somewhat from the overall left-twisted trend. The cytoplasmic and extracellular surfaces are at the top and bottom of the bundle, respectively. See the legend to Figure 4 for a further explanation.

these two transition dipoles falls within the range of observations if the experimental errors are taken into account (Urabe et al., 1989). For distinction, in Figure 4 the all-trans bundle is portrayed in green and its lysine-retinal in red, and the 13-cis bundle portrayed in yellow and its lysine-retinal in purple. It is widely believed that the retinal chromophore of bR has little motion during the photocycle of light-adapted bR. It should be pointed out, however, that this view is based upon the fact that only a trivial change in the orientation of the retinal transition dipole has been observed during photoisomerization of bR (Urabe et al., 1989). According to the results described here, however, the insignificant change in the orientation of the retinal transition dipole does not necessarily mean significant movement has not occurred in the retinal chromophore. For example, as noted above, the β-ionone ring undergoes a considerable perturbation in its position although the retinal transition dipole changes only slightly in its overall orientation, a feature that is entirely consistent with observed results. This finding provides an alternative view as to the possible motion of retinal chromophore, which may yield new insights for studies of the mechanism of bR action, especially as the motion of the chromophore plays a role in the light-driven proton pumping process.

Analysis of energy

After energy optimization, the total conformational energy E^{tot} for the all-trans bundle is -918.30 kcal/mol, and that for the 13-cis bundle is -907.82 kcal/mol; i.e., the all-trans bundle is about 10 kcal/mol lower in conformational energy than the 13-cis bundle. As defined in Equation 6, the total conformational energy of a 7-helix bundle is the sum of the total intrachain energy and the total interchain energy. From Table 3 we can see that the total intrachain energies for the all-trans and 13-cis bundles are -448.91 kcal/mol and -529.27, respectively; i.e., the former is higher than the latter by about 80 kcal/mol. Therefore, the total conformational energy in favor of the all-trans bundle is due to the total interchain energy for which the all-trans bundle is about 90 kcal/mol lower than the 13-cis bundle (Table 3).

Caution must be used in comparing the energy of the 13-cis bundle with that of the all-trans bundle. This is due to the fact that in the all-trans bundle the retinal-Lys 216 Schiff base is protonated ($-NH^+=$), and the carboxyl group of Asp 85 is deprotonated (Asp^- 85), but in the 13-cis bundle both groups are in their corresponding neutral forms ($-N=$ and Asp 85, respectively). Therefore, in addition to the conformational energy difference between the all-trans and 13-cis bundles, account must also be taken of the deprotonation and protonation energies of the protonated retinal-Lys 216 Schiff base and the ionized Asp 85, respectively. The protonation/deprotonation energy term ΔE^{prot} can be estimated from the appropriate pK_a's for the two groups, although it must be recognized the energies obtained in this way are Gibbs free energies and not potential energies. Accordingly, the real energy difference between the all-trans and 13-cis bundles should be expressed as

$$\Delta E = E_{cis} - E_{trans} = (E_{cis}^{conf} - E_{trans}^{conf}) + (E_{cis}^{prot} - E_{trans}^{prot}) = \Delta E^{conf} + \Delta E^{prot}, \quad (8)$$

where the subscripts *trans* and *cis* represent the all-trans bundle and the 13-cis bundle, and the superscripts *conf* and *prot* are used to refer to the conformational energy and protonation/deprotonation energy, respectively. Based on the relevant equilibrium constants, i.e., $pK_a = 4.3$ for the carboxyl group of aspartic acid and $pK_a = 10.5$ for the amino group of lysine (Bohinski, 1987), it can be estimated that $\Delta E^{prot} = E_{cis}^{prot} - E_{trans}^{prot} \approx 9$ kcal/mol. Substituting this value together with $\Delta E^{conf} \approx 10$ kcal/mol as derived from Table 3 into Equation 8, we obtain $\Delta E \approx 19$ kcal/mol, i.e., the 13-cis bundle is about 19 kcal/mol higher in energy than the all-trans bundle. Such an energy difference is rational, as can be illustrated as follows.

As is well known, all-trans bR, after absorbing a photon of wavelength $\lambda = 570$ nm (Mathies et al., 1991), becomes converted to 13-cis bR. Energy conservation requires that ΔE should be less than the energy of the absorbed photon. According to the Einstein equation for photon energy (see, e.g., Shankar, 1980), the energy possessed by a photon of 570 nm light is equal to $hc/\lambda \approx 50$ kcal/mol, where h is Planck's constant, and c the speed of light. Accordingly, the energy of the absorbed photon is more than sufficient to drive the all-trans $\Rightarrow$ 13-cis isomerization process.

As shown in Table 2, most of the interchain energy is contributed from helix pairs in which the two helices are very close (i.e., $D \leq 11$ Å), such as the A–B, B–C, B–G, C–D, D–E, E–F, F–G, G–A pairs in the all-trans and 13-cis bundles. Among these helix pairs, only the G–A helix pair is nearly parallel (Fig. 5), and hence its interchain electrostatic energy E_{inter}^{ES} is considerably higher than the others due to less favorable interaction of the helix macrodipoles, in agreement with the results of earlier analyses of the interactions of pairs of α-helices (Wada, 1976; Hol et al., 1978; Sheridan et al., 1982).

It is obvious that in any system consisting of seven helices the maximum number with which the antiparallel adjacent helix pairs can be formed is six. Now it seems understandable from the energetic point of view why in the 7-helix bundle structure six adjacent helix pairs are nearly antiparallel although they are inevitably mixed with one adjacent parallel pair. The question then arises:

why are the helices in the only adjacent parallel pair, i.e., helices A and G in the current case, not separated far away from each other to weaken their unfavorable parallel dipole-dipole interaction? If so, it would indeed reduce the unfavorable electrostatic energy somewhat but at the cost of losing the favorable nonbonded interchain energy that comes from the close packing of the two helices. The nonbonded interchain energies for the G-A pair in the all-trans and 13-cis bundles are −36.89 kcal/mol and −25.40 kcal/mol, respectively, which are in magnitude much greater than the corresponding electrostatic interchain energies 5.44 kcal/mol and 5.10 kcal/mol. In other words, by separating the parallel A-G helix pair, the energy gained in the electrostatic interaction is not enough to compensate the energy lost in the nonbonded interaction. The argument concerning stabilization of parallel helix pairs in helix bundles has also been addressed by Furois-Corbin and Pullman (1986) for poly-

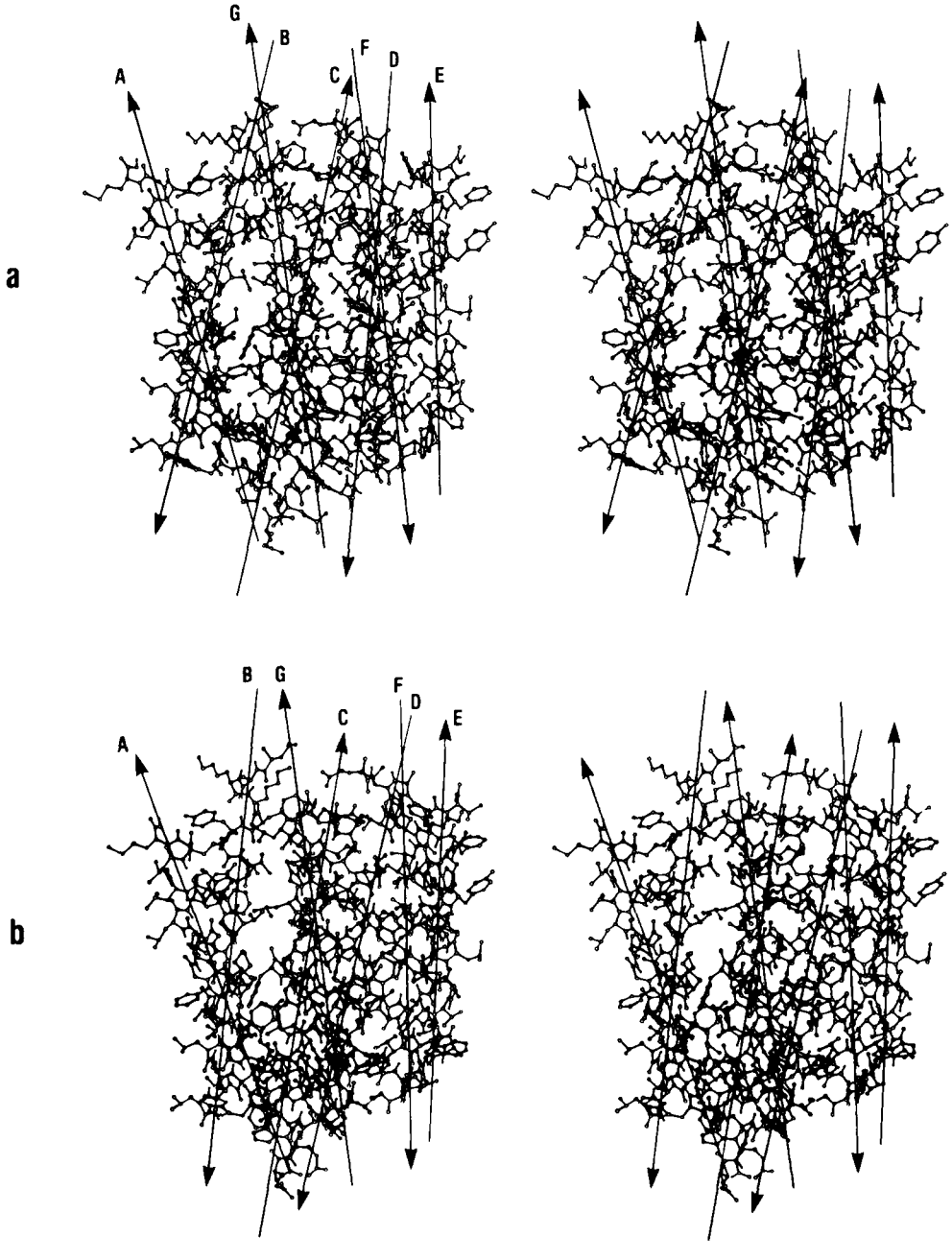

Fig. 6. The stereo stick-ball drawings for the same structures as in Figure 5 but with all heavy atoms included to show that the seven helices in both bundles are closely packed.

alanine bundles. A further discussion concerning the optimal geometrical arrangement in a 7-helix bundle will be given in the section Relation of 7-helix bundle with 4-helix bundle, where the role of left-twisted 4-helix bundles in stabilizing the 7-helix bundle will be illustrated.

Generally speaking, for the helix pairs listed in Table 2, the greater the number of atom pairs in contact the lower the interchain energy; this is, however, not always true. For example, the number of atom pairs in contact between helices B and C in the all-trans bundle is less than that in the 13-cis bundle by 10 (= 284 − 274), but the interchain energy of the former is lower than that of the latter by about 7 (≈ −46.73 − (−53.44)) kcal/mol. This once again indicates that although geometrical modeling about packing preferences based on contact surfaces leads to useful insights (Chothia & Finkelstein, 1990), it is necessary to compute the energies of various packed structures in order to assess their relative stabilities. Figure 6 illustrates the close packing of the helices in the all-trans and 13-cis bundles.

Residue number in each individual helix

In the all-trans bundle determined by high-resolution electron cryomicroscopy, the residue number of each helix was assigned (Henderson et al., 1990). If $(\phi, \psi) = (-68 \pm 20°, -38 \pm 20°)$ are defined as the dihedral angle region for helices (Chou et al., 1984), it was found after energy optimization that the majority of residues assigned by Henderson et al. (1990) as helix components remained in the helix region except those residues located around the two ends of helices C and D and N-terminus of helix A and N-terminus of helix E. For those residues, in contrast to the original assignment, it was observed that some of them moved out from the helix region, whereas some of them moved into the helix region from nonhelix region, as shown in Figure 1 and Table 4. Such a modification is reasonable because, as claimed by Henderson et al. (1990), the residue number at which each helix terminates as assigned by them is uncertain at the top and bottom of each helix by at least 1 residue.

Table 4. *Helix parameters*

	All-trans bundle determined by Henderson et al. (1990)		Energy-optimized all-trans bundle		Energy-optimized 13-cis bundle	
Helix	Residues	Number	Residues	Number	Residues	Number
A	10-32	23	11-32	22	10-32	23
B	38-62	25	38-62	25	38-62	25
C	80-101	22	76-99	24	76-100	25
D	108-127	20	107-126	20	107-126	20
E	136-157	22	138-157	20	138-157	20
F	167-193	27	167-193	27	167-193	27
G	203-227	25	203-227	25	203-227	25

Microenvironment of retinal chromophore

The retinal chromophore, which is vital to bR functioning as a light-driven proton pump, is bound to Lys 216 of bR via a Schiff-base linkage. Driven by light absorption, bR undergoes a rapid conformational change during which the retinal chromophore is converted from the all-trans to the 13-cis isomer, with its β-ionone ring moving a vertical distance of about 5.7 Å (Fig. 4), which results in proton transport across the bacterial membrane. Such a motion occurring at the center of the molecule would change not only the general conformation of the 7-helix bundle as indicated in Tables 1 and 2, but, more important, the microenvironment of the retinal chromophore as well. The change of the latter might be quite subtle for the further investigation into the proton-pumping mechanism. The microenvironment in which the retinal chromophore dwells can be effectively described in terms of the residues that are in contact with the retinal-Lys 216 of helix G but belong to the other 6 helices, as illustrated in Table 5 and Kinemage 3. As we can see from these data, the retinal-Lys 216 in the all-trans bundle is in contact with all the other six helices, namely, helices A, B, C, D, E, and F. However, the retinal-Lys 216 in the 13-cis bundle is in contact with only five helices, i.e., helices B, C, D, E, and F. The corresponding residues and numbers of atom pairs in contact with the retinal-Lys 216 are also listed in Table 5. These data provide us with a detailed picture about the microenvironmental change around the retinal chromophore when the all-trans bundle is converted to the 13-cis bundle. This change reflects the local rearrangements of the protein residues in the chromophore-binding pocket, which was thought of as "functionally important motions" as discussed by Ansari et al. (1985) and Frauenfelder et al. (1988).

Listed in Table 6 are the interaction (both electrostatic and nonbonded) energies between retinal-Lys 216 of helix G and each of the other helices in the all-trans and 13-cis bundles, respectively. We can see from the table that the interactions of retinal-Lys 216 with helices C and F are much stronger than those with the other helices. This is an instructive finding because most functionally important residues, such as Asp 85, Asp 96, and Tyr 185, are located in helices C and F (Khorana, 1988; Mogi et al., 1988). The strong interaction energies between retinal-Lys 216 and these two helices reflect a strong coupling of retinal chromophore with these residues, which are directly associated with the proton-pumping mechanism of bR. Furthermore, a remarkably strong electrostatic interaction has been observed between retinal-Lys 216 and helix C in the all-trans bundle. This is due to the ionic interaction between the protonated Schiff base in retinal-Lys 216 (Krt^+ 216) and the deprotonated Asp^- 85 in helix C.

Table 5. *Residues that contact with the retinal-Lys 216 of helix G in the energy-optimized bundles*

	All-trans bundle			13-Cis bundle		
Helix	Residue in contact	Number of atom pairs in contact	Subtotal atom pairs in contact	Residue in contact	Number of atom pairs in contact	Subtotal atom pairs in contact
A	Met 20	16	16			0
B	Ala 53	2	4	Ala 53	9	15
	Tyr 57	2		Tyr 57	6	
C	Asp 85	3	90	Asp 85	6	77
	Trp 86	40		Trp 86	30	
	Thr 89	30		Thr 89	12	
	Thr 90	4		Thr 90	14	
	Leu 93	13		Leu 93	14	
				Leu 94	1	
D	Met 118	17	39	Met 118	17	17
	Gly 122	22				
E	Trp 138	3	36			53
	Ser 141	14				
	Met 145	19		Met 145	30	
				Ile 148	23	
F	Trp 182	2	110	Trp 182	28	80
	Tyr 185	43		Tyr 185	43	
	Pro 186	21		Pro 186	9	
	Trp 189	44				
Total atom pairs in contact			295			242

Table 6. *Interaction energies of retinal-Lys 216 of helix G with helices A, B, ..., F, respectively*

	All-trans bundle, interaction energy (kcal/mol)			13-Cis bundle, interaction energy (kcal/mol)		
Helix	ϵ_{ES}[a]	ϵ_{NB}[b]	ϵ[c]	ϵ_{ES}[a]	ϵ_{NB}[b]	ϵ[c]
A	0.52	−2.15	−1.63	0.17	−1.38	−1.21
B	0.26	−2.13	−1.87	−0.20	−3.87	−4.07
C	−31.01	−15.32	−46.32	0.08	−14.61	−14.53
D	−0.28	−7.97	−8.26	−0.06	−2.93	−2.99
E	1.13	−4.85	−3.72	0.12	−5.70	−5.58
F	−1.05	−18.43	−19.48	−0.24	−15.46	−15.70

[a] ϵ_{ES} is the electrostatic interaction energy between the retinal-Lys 216 and the helix of column 1.
[b] ϵ_{NB} is the nonbonded interaction energy between the retinal-Lys 216 and the helix of column 1.
[c] $\epsilon = \epsilon_{ES} + \epsilon_{NB}$.

When the all-trans bundle is converted to the 13-cis bundle, it can be derived from Table 6 that the total interaction energy between the retinal-Lys 216 of helix G and all the other helices would change from −81.28 kcal/mol to −44.08 kcal/mol, indicating that such a conversion would relax the coupling interaction of retinal chromophore with its microenvironment. This is fully consistent with the results of Table 5, where the total number of atom pairs in contact between the retinal-Lys 216 and all the other helices in the all-trans bundle is 295, whereas that in the 13-cis bundle is reduced to 242. Such an interesting finding is also inconsistent with the fact that an absorption of a photon with a wavelength of 570 nm is needed to convert the all-trans bR to the 13-cis bR as discussed in Analysis of energy. However, it is not clear yet how such a relaxation in interaction energy is related to the proton-pumping mechanism of bR.

Relation of 7-helix bundle with 4-helix bundle

It is instructive to examine the relationship between the 7-helix bundle membrane-bound protein obtained here and the 4-helix bundles observed in a number of soluble proteins. In most of the observed 4-helix bundle proteins (Argos et al., 1977; Weber & Salemme, 1980; Richardson, 1981; Sheridan et al., 1982; Abdel-Meguid et al., 1987) the four α-helices form an assembly with an approximately square cross section, and the orientation angle between neighboring helices (defined by Equation 5) is nearly constant, with a value of $\Omega_0 = -162° \pm 6°$ (see Fig. 1 of Sheridan et al. [1982] or Chou et al. [1988]), so that the whole structure assumes an overall antiparallel left-twisted bundle conformation. It has been shown that such a packing arrangement is energetically the most favorable (Chou et al., 1988; Carlacci & Chou, 1990; Carlacci et al., 1991a). Interestingly, from Table 2, Figure 5,

and Kinemage 1 we find that these features of left-twisted 4-helix bundles also exist in the all-trans and 13-cis 7-helix bundles, as can be seen through the schemes presented in Equations 9 and 10 (below), where ABCG-bundle represents the 4-helix bundle consisting of helices A, B, C, G, and it is followed by the values of the four orientation angles between its successive adjacent helices, e.g., −150° is the value of the orientation angle Ω_0 between helices A and B in the all-trans bundle, and so forth. When the directionality of the axis of the individual helix is not of interest, the value of an orientation angle Ω in a bundle can also be expressed by $\Omega^0 \pm 180°$ (Sheridan et al., 1982), as shown in the parentheses of Equations 9 and 10. From the above grouped data we can see: helices B, C, F, G in both the all-trans and 13-cis bundles forms a typical antiparallel left-twisted 4-helix bundle as observed in most of the observed 4-helix proteins; helices A, B, C, G and helices C, E, F, G each form a mixed left-twisted 4-helix bundle, in which two adjacently antiparallel helix pairs are mixed with two adjacently parallel helix pairs but the whole structure is left-twisted; and helices C, D, E, F form an antiparallel quasi-left-twisted 4-helix bundle, in which one orientation angle, i.e., the one between helices C and D, deviates somewhat from the overall left-twisted trend. This provides useful insights that will be of value in further modeling other 7-helix proteins by suggesting that many 7-helix membrane proteins, such as serotonin and dopamine receptors, might probably be built up on a stepwise fashion based on 4-helix bundle groups.

Work ahead

The all-trans and 13-cis bundle structures reported here were calculated in terms of ECEPP potential. As reported in a recent paper by Roterman et al. (1989), a comparison of the CHARMM (Brooks et al., 1983), AMBER (Weiner & Kollman, 1981), and ECEPP potentials for peptides has indicated that the ECEPP potential is a very good one, and its restriction on bond lengths and bond angles is also an appropriate approximation for polypeptides. Nevertheless, it would be interesting to know what structures will be obtained if the calculation is carried out in the CHARMM or AMBER system.

Furthermore, all calculations in this paper were carried out in the absence of explicit solvent molecules. In vivo, the protein is surrounded by water. The validity of ECEPP in dealing with polypeptides without explicitly including solvent molecules has been discussed by Roterman et al. (1989). As a matter of fact, in the ECEPP algorithm an "effective dielectric constant" D is taken as 2 for all calculations (Momany et al., 1975). The value of 2 for D was obtained by analysis of CNDO/2 calculations (McGuire et al., 1972) on hydrogen-bonded dimers. Actually, the use of the effective dielectric constant $D = 2$ is operationally equivalent to the experimental dielectric constant of $D \sim 4$ for polypeptides in polar media (Momany et al., 1975). Therefore, except for a very small percentage of superficial groups that are directly exposed to the solvent, the treatment by using an effective dielectric constant as done in ECEPP is a reasonably good approximation. This has also been supported by the fact that the recently predicted antifreeze protein structure (Chou, 1992) and bovine somatotropin structure (Carlacci et al., 1991a), both of which were computed based on the ECEPP algorithm, are excellently consistent with the relevant experimental observations. However, it would provide many insights into the proton-translocation channel in bR and its action mechanism if calculations can be made in the presence of explicit solvent molecules although it is quite difficult yet to do so.

It should be pointed out that, besides Asp 85 and the Schiff base, some other charged residues in bR could also be protonated or deprotonated (Gerwert, 1989) during the proton-pumping process. However, in our calculations, the effects of protonation or deprotonation for those residues were omitted. Because the current computation is focused on the overall structure, especially the packing structure in the 7-helix bundle, such an approximate treatment is valid. However, if the similar effects can be taken into account for all possibly protonated and deprotonated residues, a lot of local, detailed information will be provided that would be very useful for investigating the proton-pumping mechanism of bR at a deeper level.

Finally, the current calculations were carried out in the absence of loops. Such a simplified model is justified by the fact that the starting point for energy optimization

ABCG-bundle:	−150°;	−170°;	21°(−159°);	10°(−170°)	}	
BCFG-bundle:	−170°;	−158°;	−165°;	−158°		
CDEF-bundle:	168°;	−151°;	−169°;	−158°		in the all-trans bundle; (9)
CEFG-bundle:	23°(−157°);	−169°;	−165°;	21°(−159°)	}	

ABCG-bundle:	−154°;	−169°;	18°(−162°);	16°(−164°)	}	
BCFG-bundle:	−169°;	−163°;	−162°;	−165°		
CDEF-bundle:	170°;	−167°;	−170°;	−163°		in the 13-cis bundle, (10)
CEFG-bundle:	10°(−170°);	−170°;	−162°;	18°(−162°)	}	

was based on the electron-diffraction structure (Henderson et al., 1990) that does not include loops either. Furthermore, previous studies (Chou et al., 1983, 1984, 1985, 1986, 1988, 1990) have indicated that many important packing features between secondary structures in proteins can be predicted by energy minimization without the presence of loops. However, the inclusion of loops in the calculation would not only make the model more realistic but also further improve the calculated results (Carlacci & Chou, 1990), especially in more accurately predicting the conformations of residues that are located at the two ends of the helices.

Therefore, the present calculations should be regarded as a prelude to a series of further calculations that will be carried out under the condition of explicitly containing water molecules, or counting the effects of all possibly protonated and deprotonated residues, or including the loop component, or a combination of all these factors.

Conclusion

By means of a combination of simulated annealing and energy minimization, the three-dimensional structure of the all-trans bundle of bR has been refined and that of the 13-cis bundle predicted. The heavy-atom rms deviation between the refined all-trans bundle and that determined by Henderson et al. (1990) is 1.6 Å, whereas the corresponding rms value between the refined all-trans bundle and the predicted 13-cis bundle is 2.4 Å. A comparison of the all-trans and 13-cis bundles indicates that during their interconversion the β-ionone ring of retinal moves about 5.6 Å in a direction perpendicular to the membrane plane. Although this represents a significant structural perturbation of the region surrounding the chromophore, the retinal transition dipole undergoes only a slight change during the structural transition, which is fully in accord with experimental observations (Heyn et al., 1977; Lin & Mathies, 1989). Thus, the small change in the orientation of the retinal transition dipole does not necessarily imply that significant movement does not occur in the retinal chromophore. This finding provides an alternative to the view which assumes that the retinal chromophore remains essentially unchanged during the all-trans ⇒ 13-cis photoisomerization.

The left-handed twisted character observed in most four-helix bundle proteins also appears in 4-helical subbundles in both the all-trans and 13-cis bundles, suggesting that a stepwise strategy may be employed as a means of building up the three-dimensional structure of other 7-helix bundle membrane proteins, an approach that would significantly reduce the space that must be searched by simulated annealing and gradient-base energy minimization methods.

The energy of the all-trans bundle is about 10 kcal/mol lower than that of the 13-cis bundle. On the other hand, owing to the different protonated states at the Schiff base and the carboxyl group of Asp 85, there is an additional protonation/deprotonation energy (~9 kcal/mol) in favor of the all-trans bundle. Therefore, the total energy of all-trans bundle is lower than that of cis-bundle by about 19 kcal/mol, an energy difference that is less than the energy (~50 kcal/mol) of the 570-nm photon, which drives the photoisomerization of the all-trans to 13-cis bR, fully fitting into the energetic requirement from a kinetic point of view.

The internal movement of the β-ionone ring brings about a change in the microenvironment surrounding the chromophore such that the number of atom pairs in contact between the retinal-Lys 216 of helix G and the six other helices is reduced from 295 to 242. As a result of that, the coupling interaction of the retinal-Lys 216 on helix G with the other helices is weakened by about 37 kcal/mol when the all-trans bundle is converted to the 13-cis bundle, indicating a change of the coupling strength of the chromophore with its binding pocket. Such a relaxation in coupling strength is no doubt important to the proton-pumping function of bR although its mechanism is not clear yet. Furthermore, for both all-trans and 13-cis bundles, the interaction energies of retinal-Lys 216 with helices C and F are much stronger than those with the other helices. This is an instructive finding because most functionally important residues, such as Asp 85, Asp 96, and Tyr 185, are located in helices C and F. The strong interaction energies between retinal-Lys 216 and these two helices reflect a strong coupling of retinal chromophore with these functionally important residues. Analysis of these coupling interactions and their intrinsic relationship with the proton-pumping mechanism of bR is certainly worthy of further consideration.

Acknowledgment

We express our gratitude to Dr. C.D. Strader for valuable discussions.

References

Abdel-Meguid, S.S., Shieh, H.S., Smith, W.W., Dayringer, H.E., Violand, B.N., & Bentle, L.A. (1987). Three-dimensional structure of a genetically engineered variant of porcine growth hormone. *Proc. Natl. Acad. Sci. USA 84*, 6434–6437.

Ansari, A., Berendzen, J., Bowne, S.F., Frauenfelder, H., Iben, I.E.T., Sauke, T.B., Shyamsunder, E., & Young, R.D. (1985). Protein states and proteinquakes. *Proc. Natl. Acad. Sci. USA 82*, 5000–5004.

Argos, P., Rossmann, M.G., & Johnson, J.E. (1977). A four-helical super-secondary structure. *Biochem. Biophys. Res. Commun. 75*, 83–86.

Boehm, M.F., Gawinowicz, M.A., Foucault, A., Derguini, F., & Nakanishi, K. (1990). Photoaffinity labeling studies of bacteriorhodopsin with [15-^{3}H]-3-diazo-4-keto-all-trans-retinal. *J. Am. Chem. Soc. 112*, 7779–7782.

Bohinski, R.C. (1987). *Modern Concepts in Biochemistry*, 5th Ed., p. 76. Allyn and Bacon, Inc., Boston.

Brooks, B.R., Bruccoleri, R.E., Olafson, B.D., States, D.J., Swaminathan, S., & Karplus, M.J. (1983). CHARMM: A program for macromolecular energy, minimization, and dynamics calculations. *J. Comp. Chem. 4*, 187-217.

Carlacci, L. & Chou, K.-C. (1990). Energetic approach to the folding of four α-helices connected sequentially. *Protein Eng. 3*, 509-514.

Carlacci, L. & Chou, K.-C. (1991). New development on energetic approach to the packing in proteins. *J. Comp. Chem. 12*, 410-415.

Carlacci, L., Chou, K.-C., & Maggiora, G.M. (1991a). A heuristic approach to predicting the tertiary structure of bovine somatotropin. *Biochemistry 30*, 4389-4398.

Carlacci, L., Schulz, M.W., & Chou, K.-C. (1991b). Geometric and energetic parameters in lysine-retinal chromophores. *Protein Eng. 4*, 885-889.

Chothia, C. & Finkelstein, A.V. (1990). The classification and origins of protein folding patterns. *Annu. Rev. Biochem. 59*, 1007-1039.

Chothia, C., Levitt, M., & Richardson, D. (1977). Structure of proteins: Packing of α-helices and pleated sheets. *Proc. Natl. Acad. Sci. USA 74*, 4130-4134.

Chothia, C., Levitt, M., & Richardson, D. (1981). Helix to helix packing in proteins. *J. Mol. Biol. 145*, 215-250.

Chou, K.-C. (1992). Energy-optimized structure of antifreeze protein and its binding mechanism. *J. Mol. Biol. 223*, 509-517.

Chou, K.-C. & Carlacci, L. (1991). Simulated annealing approach to the study of protein structures. *Protein Eng. 4*, 661-667.

Chou, K.-C. & Maggiora, G.M. (1988). Biological function of low-frequency vibrations (phonons). 7. The impetus for DNA to accommodate intercalators. *Br. Polym. 20*, 143-148.

Chou, K.-C., Maggiora, G.M., Némethy, G., & Scheraga, H.A. (1988). Energetics of the structure of the four-α-helix bundle in proteins. *Proc. Natl. Acad. Sci. USA 85*, 4295-4299.

Chou, K.-C. & Mao, B. (1988). Collective motion in DNA and its role in drug intercalation. *Biopolymers 27*, 1795-1815.

Chou, K.-C., Némethy, G., Rumsey, S., Tuttle, R.W., & Scheraga, H.A. (1985). Interactions between an α-helix and a β-sheet: Energetics of α/β packing in proteins. *J. Mol. Biol. 186*, 591-609.

Chou, K.-C., Némethy, G., Rumsey, S., Tuttle, R.W., & Scheraga, H.A. (1986). Interactions between two β-sheets: Energetics of β/β packing in proteins. *J. Mol. Biol. 188*, 641-649.

Chou, K.-C., Némethy, G., & Scheraga, H.A. (1983). Energetic approach to the packing of α-helices. 1. Equivalent helices. *J. Phys. Chem. 87*, 2869-2881.

Chou, K.-C., Némethy, G., & Scheraga, H.A. (1984). Energetic approach to the packing of α-helices. 2. General treatment of nonequivalent and nonregular helices. *J. Am. Chem. Soc. 106*, 3161-3170.

Chou, K.-C., Némethy, G., & Scheraga, H.A. (1990). Energetics of interactions of regular structural elements in proteins. *Acc. Chem. Res. 23*, 134-141.

Ding, W.D., Tsipouras, A., Ok, H., Tamamoto, T., Gawinowicz, M.A., & Nakanishi, K. (1990). Photoaffinity labeling of bacteriorhodopsin. *Biochemistry 29*, 4898-4904.

Dixon, R.A.F., Sigal, I.S., & Strader, C.D. (1988). Structure-function analysis of the β-adrenergic receptor. *Cold Spring Harbor Symp. Quant. Biol. 53*, 487-497.

Earnest, T.N., Roepe, P., Braiman, M.S., Gillespie, J., & Rothschild, K.J. (1986). Orientation of the bacteriorhodopsin chromophore probed by polarized Fourier transform infrared difference spectroscopy. *Biochemistry 25*, 7793-7798.

Engelman, D.M., Henderson, R., McLachlan, A.D., & Wallace, B.A. (1980). Path of the polypeptide in bacteriorhodopsin. *Proc. Natl. Acad. Sci. USA 77*, 2023-2027.

Engelman, D.M. & Zaccai, G. (1980). Bacteriorhodopsin is an inside-out protein. *Proc. Natl. Acad. Sci. USA 77*, 5894-5898.

Fahmy, K., Siebert, F., Grossjean, M.F., & Tavan, P. (1989). Photoisomerization in bacteriorhodopsin studied by linear dichroism, and photoselection experiments combined with quantum chemical theoretical analysis. *J. Mol. Struct. 214*, 257-288.

Fodor, S.P.A., Ames, J.B., Gebhard, R., van der Berg, E.M.M., Stoeckenius, W., Lugtenburg, J., & Mathies, R.A. (1988). Chromophore structure in bacteriorhodopsin's N intermediate: Implications for the proton-pumping mechanism. *Biochemistry 27*, 7097-7101.

Frauenfelder, H., Parak, F., & Young, R.D. (1988). Conformational substates in proteins. *Annu. Rev. Biophys. Biophys. Chem. 17*, 451-479.

Furois-Corbin, S. & Pullman, A. (1986). Theoretical study of the packing of α-helices of poly(L-alanine) into transmembrane bundle. Possible significance for ion-transfer. *Biochim. Biophys. Acta 860*, 165-177.

Gebhard, F.X., Schertler, F.X., Lozier, R., Michel, H., & Oesterhelt, D. (1991). Chromophore motion during the bacteriorhodopsin photocycle: Polarized absorption spectroscopy of bacteriorhodopsin and its M-state bacteriorhodopsin crystals. *EMBO J. 10*, 2353-2361.

Gerwert, K., Hess, B., Soppa, J., & Oesterhelt, D. (1989). Role of aspartate-96 in proton translocation by bacteriorhodopsin. *Proc. Natl. Acad. Sci. USA 86*, 4943-4947.

Harbison, G.S., Smith, S.O., Pardoen, J.A., Courtin, J.M., Lugtenburg, J., Herzfeld, J., Mathies, R.A., & Griffin, R.G. (1985). Solid-state ^{13}C NMR detection of a perturbed 6-*s*-trans chromophore in bacteriorhodopsin. *Biochemistry 24*, 6955-6962.

Henderson, R., Baldwin, J.M., Ceska, T.A., Zemlin, F., Beckmann, E., & Downing, K.H. (1990). Model for the structure of bacteriorhodopsin based on high-resolution electron cryo-microscopy. *J. Mol. Biol. 213*, 899-929.

Heyn, M.P., Cherry, R.L., & Muller, U. (1977). Transient and linear dichroism studies on bacteriorhodopsin: Determination of the orientation of the 568 nm all-trans retinal chromophore. *J. Mol. Biol. 117*, 607-620.

Hol, W.G.J., van Duijnen, P.T., & Berendsen, H.J.C. (1978). The α-helix dipole and the properties of proteins. *Nature 273*, 443-446.

Howe, W.J., Blinn, J.R., Moon, J.B., Hagadone, T.R., White, G.J., & Schultz, M.W. (1992). MOSAIC: A distributed software system for molecular modeling of small molecules and macromolecules. *J. Comp. Chem.* (in press).

Khorana, H.G. (1988). Bacteriorhodopsin, a membrane protein that uses light to translocate protons. *J. Biol. Chem. 263*, 7439-7442.

Khorana, H.G., Gerber, G.E., Herlihy, W.C., Gray, C.P., Anderegg, R.J., Nihei, K., & Biemann, K. (1979). Amino acid sequence of bacteriorhodopsin. *Proc. Natl. Acad. Sci. USA 76*, 5046-5050.

Kouyama, T., Nasuda-Kouyama, A., Ikegami, A., Mathew, M.K., & Stoeckenius, W. (1988). Bacteriorhodopsin photoreaction: Identification of a long-lived intermediate N (P, R_{350}) at a high pH and its M-like photoproduct. *Biochemistry 27*, 5855-5863.

Lin, S.W. & Mathies, R.A. (1989). Orientation of the protonated retinal Schiff base group in bacteriorhodopsin from absorption linear dichroism. *Biophys. J. 56*, 653-660.

Lozier, R.H., Bogomolni, R.A., & Stoeckenius, W. (1975). Bacteriorhodopsin: A light-driven proton pump in *Halobacterium halobium*. *Biophys J. 15*, 955-962.

Mathies, R.A., Lin, S.W., Ames, J.B., & Pollard, W.T. (1991). From femtoseconds to biology: Mechanism of bacteriorhodopsin's light-driven proton pump. *Annu. Rev. Biophys. Biophys. Chem. 20*, 491-518.

McGuire, R.F., Momany, F.A., & Scheraga, H.A. (1972). Energy parameters in polypeptides. 5. An empirical hydrogen bond potential function based on molecular orbital calculations. *J. Phys. Chem. 76*, 375-384.

Mogi, T., Stern, L.J., Marti, T., Chao, B.H., & Khorana, H.G. (1988). Aspartic acid substitutions affect proton translocation by bacteriorhodopsin. *Proc. Natl. Acad. Sci. USA 85*, 4148-4152.

Momany, F.A., McGuire, R.F., Burgess, A.W., & Scheraga, H.A. (1975). Energy parameters in polypeptides. 7. Geometrical parameters, partial atomic charges, nonbonded interactions, hydrogen bond interactions, and intrinsic torsional potentials for the naturally occurring amino acids. *J. Phys. Chem. 79*, 2351-2381.

Nagle, J.F., Parodi, L.A., & Lozier, R.H. (1982). Procedure for testing kinetic models of the photocycle of bacteriorhodopsin. *Biophys. J. 38*, 161-174.

Némethy, G., Pottle, M.S., & Scheraga, H.A. (1983). Energy parameters in polypeptides. 9. Updating of geometrical parameters, nonbonded interactions, and hydrogen bond interactions for the naturally occurring amino acids. *J. Phys. Chem. 87*, 1883-1887.

Oesterhelt, D. & Stoeckenius, W. (1973). Functions of a new photoreceptor membrane. *Proc. Natl. Acad. Sci. USA 70*, 2853-2857.

Ovchinnikov, Y.A. (1982). Rhodopsin and bacteriorhodopsin: Structure-function relationships. *FEBS Lett. 148*, 179-190.

Ovchinnikov, Y.A., Abdulaev, N.G., Feigina, M.Y., Kiselev, A.V., & Lobanov, N.A. (1979). The structural basis of the functioning of bacteriorhodopsin: An overview. *FEBS Lett. 100*, 219–224.

Parodi, L., Lozier, R.H., Nagle, J.F., Bogomolni, R.A., Wolber, P.K., Mowery, P.C., & Stoeckenius, W. (1980). Chromophore orientation in dark- and light-adapted purple membrane. *Fed. Proc. 39*, 1264.

Pople, J.A., Beveridge, D.L., & Dobosh, P.A. (1967). Approximate self-consistent molecular-orbital theory. 5. Intermediate neglect of differential overlap. *J. Chem. Phys. 47*, 2026–2033.

Popot, J.L., Engelman, D.M., Gurel, O., & Zaccaï, G. (1989). Tertiary structure of bacteriorhodopsin. *J. Mol. Biol. 210*, 829–847.

Rao, J.K.M., Hargrave, P.A., & Argos, P. (1983). Will the seven-helix bundle be a common structure for integral membrane proteins? *FEBS Lett. 156*, 165–169.

Richardson, J.S. (1981). The anatomy and taxonomy of protein structure. *Adv. Protein Chem. 34*, 167–339.

Ridley, J.E. & Zener, M.C. (1973). Intermediate neglect of differential overlap (INDO) technique for spectroscopy. Pyrrole and the azines. *Theor. Chim. Acta 32*, 111–134.

Roterman, I.K., Lambert, M.H., Gibson, K.D., & Scheraga, H.A. (1989). A comparison of the CHARMM, AMBER and ECEPP potentials for peptides. II. ϕ–ψ maps for *N*-acetyl alanine *N'*-methyl amide: Comparison, contrasts and simple experimental tests. *J. Biomol. Struct. Dynam. 7*, 421–453.

Schulton, K. & Tavan, P. (1978). A mechanism for the light-driven proton pump of *Halobacterium halobium*. *Nature 272*, 85–86.

Shankar, R. (1980). *Principles of Quantum Mechanics*, p. 115. Plenum Press, New York.

Sheridan, R.P., Levy, R.M., & Salemme, F.R. (1982). α-Helix dipole model and electrostatic stabilization of 4-α-helical proteins. *Proc. Natl. Acad. Sci. USA 79*, 4545–4549.

Strader, C.D., Sigal, I.S., & Dixon, R.A.F. (1989). Structural basis of β-adrenergic receptor function. *FASEB J. 3*, 1825–1832.

Urabe, H., Otomo, J., & Ikegami, A. (1989). Orientation of retinal in purple membrane determined by polarized Raman spectroscopy. *Biophys. J. 56*, 1225–1228.

Vásquez, M., Némethy, G., & Scheraga, H.A. (1983). Computed conformational states of the 20 naturally occurring amino acid residues and of the prototype residue α-aminobutyric acid. *Macromolecules 16*, 1043–1049.

Wada, A. (1976). α-Helix as an electric macro-dipole. *Adv. Biophys. 9*, 1–63.

Weber, P.C. & Salemme, F.R. (1980). Structural and functional diversity in 4-α-helical proteins. *Nature 287*, 82–84.

Weiner, P.K. & Kollman, P.A. (1981). AMBER: Assisted model building with energy refinement. A general program for modeling molecules and their interactions. *J. Comp. Chem. 2*, 287–303.